Agenzia nazionale per le nuove tecnologie,
l'energia e lo sviluppo economico sostenibile

MINISTERO DELLO SVILUPPO ECONOMICO

Ricerca di Sistema elettrico

Sviluppo di Schemi Numerici Per l'Integrazione delle Equazioni del Modello Radiativo M1 in HeaRT

D. Cecere, E. Giacomazzi, N. Arcidiacono, F.R. Picchia

Report RdS/PAR2018/052

SVILUPPO DI SCHEMI NUMERICI PER L'INTEGRAZIONE DELLE EQUAZIONI DEL MODELLO RADIATIVO M1 IN HEART

D. Cecere, E. Giacomazzi, N. Arcidiacono, F.R. Picchia (ENEA)

Dicembre 2018

Report Ricerca di Sistema Elettrico

Accordo di Programma Ministero dello Sviluppo Economico - ENEA
Piano Annuale di Realizzazione 2018 (Estensione 2017)
Area: Generazione di energia con basse emissioni di carbonio
Progetto B.2: Polo Tecnologico del SULCIS: Tecnologie e Metodologie "Low Carbon" e Edifici ad Energia Quasi Zero (nZEB)
Obiettivo: Parte A1 - a.2 - Cicli a CO2 Supercritica
Task a.2.4 – Studi mediante Simulazione Numerica (HeaRT) di processi di ossi-combustione in atmosfera di CO2 supercritica
Responsabile del Progetto: Franca Rita Picchia, ENEA

Indice

Sommario

Nell'ambito dello studio degli effetti della radiazione termica su fiamme si è sviluppato ed implementato in HeaRT un solutore numerico stabile ed efficiente per la soluzione delle equazioni del trasferimento radiativo di energia. Il trasferimento radiativo di energia (RTE) è un meccanismo molto importante in diverse applicazioni: camere di combustione di motori ad alta pressione e ad alta temperatura, propulsione a razzo, veicoli ipersonici, rientro aerospaziale, sistemi di protezione termica, produzione di vetro, generatori di plasma e fusione nucleare. Alle temperature presenti in camera di combustione, le specie gassose che assorbono ed emettono in modo significativo sono CO_2, H_2O, CO, S_2, NO, CH_4. Altri gas, come N_2, O_2, H_2 sono trasparenti alla radiazione infrarossa e non emettono in modo significativo; tuttavia, diventano importanti assorbitori/emettitori a temperature molto elevate. Un contributo non trascurabile alle radiazioni è anche fornito da particelle di carbone ad alta temperatura (fuliggine) all'interno della fiamma e da particolato sospeso (come nella combustione di carbone polverizzato). I coefficienti di emissione e di assorbimento dei gas aumentano (di svariati ordini di grandezza) proporzionalmente alla concentrazione delle specie partecipanti e quindi alla pressione della miscela per una data frazione molare. Inoltre, i coefficienti spettrali variano con la temperatura ma anche con la pressione. Per quanto riguarda le fiamme, è noto che trascurare le radiazioni a condizioni di pressione atmosferica può portare a una sovrastima della temperatura fino a 200 K. Il trasferimento di energia radiante viene preso in considerazione per mezzo del modello diffusivo M1 brevemente descritto nel seguito. Per il momento, l'interazione radiazione di turbolenza viene trascurata, sebbene si suppone giochi un ruolo importante nel raffreddamento di fiamma alle condizioni di alta pressione. I coefficienti di assorbimento medio di Planck delle specie verranno accuratamente calcolati utilizzando i database spettroscopici ad alta risoluzione HITRAN e HITEMP. Il modello M1 è un modello di radiazione macroscopica. Dal 1978 questo modello è stato sviluppato da molti autori e si basa su equazioni di campo per l'energia radiativa e il vettore del flusso di calore radiativo. Il limite è che è valido per i media in assenza di scattering. Il vantaggio principale è che è indipendente dall'opacità del mezzo, cioè si adatta e lavora dallo spessore ottico sottile a quello spesso. Esiste anche una forma mediata del modello M1 per i flussi turbolenti anche se molto complessa e costosa da risolvere. È stata infine sviluppata una formulazione semplificata di questo modello: questo è più adatto ai problemi di combustione e quindi applicato nelle simulazioni attuali. Quando il mezzo segue la legge di Rayleigh, il modello M1, consiste in un equazione per la densità di energia Er (Jm-3):

$$\frac{\partial E_r}{\partial t} + \nabla \cdot \boldsymbol{F_r} = c(\sigma_P a T^4 - \sigma_E E_r). \tag{0.1}$$

ed una equazione di trasporto per il suo flusso F (Jm-2s-1):

$$c\frac{\partial F_r}{\partial t} + c\nabla \cdot \boldsymbol{D_r E_r} = -\sigma_F \boldsymbol{F_r}. \tag{0.2}$$

dove T è la temperatura, c la velocità della luce, σ_p il coefficiente di assorbimento medio di Planck, σ_E e σ_F i coefficienti di assorbimento effettivo, $\boldsymbol{D_r}$ il tensore di Eddington adimensionale che tiene in conto dell'effettiva opacità della fiamma. Queste 4 equazioni sono fortemente non lineari (a causa della forte non linearità del tensore di Eddington) e presentano dei termini sorgente al loro interno che le rendono particolarmente stiff. Per risolverle nel tempo in maniera stabile e con un passo temporale adeguato la discretizzazione ai volumi finiti delle precedenti equazioni (la presenza della velocità della luce nelle equazioni impone, con i classici metodi Runge-Kutta, passi temporali di $1 * 10^{-}18s$) si è reso necessario l'utilizzo di metodi IMEX-PEER (metodi implici-espliciti che trattano i termini stiff delle equazioni in modo implicito) ed il calcolo dei flussi con un solutore parziale di Riemann di tipo HLLE.

La soluzione delle equazioni del modello radiativo con la metodologia scelta, è stata applicata ad una fiamma laminare a contro-diffusione di c, (in Fig.0.2 è rappresentato il profilo di temperatura che raggiunge nella zona stechiometrica un picco di 2200 K, il CH_4 è iniettato a z = −0.005 m mentre O_2/CO_2 a z = 0.005 m con velocità negativa) e sono stati calcolati i valori di E_r e dei flussi radiativi in ogni punto della griglia computazionale. La divergenza dei flussi radiativi rappresenta il termine sorgente dell'equazione dell'energia totale rappresentato in Fig.0.1.

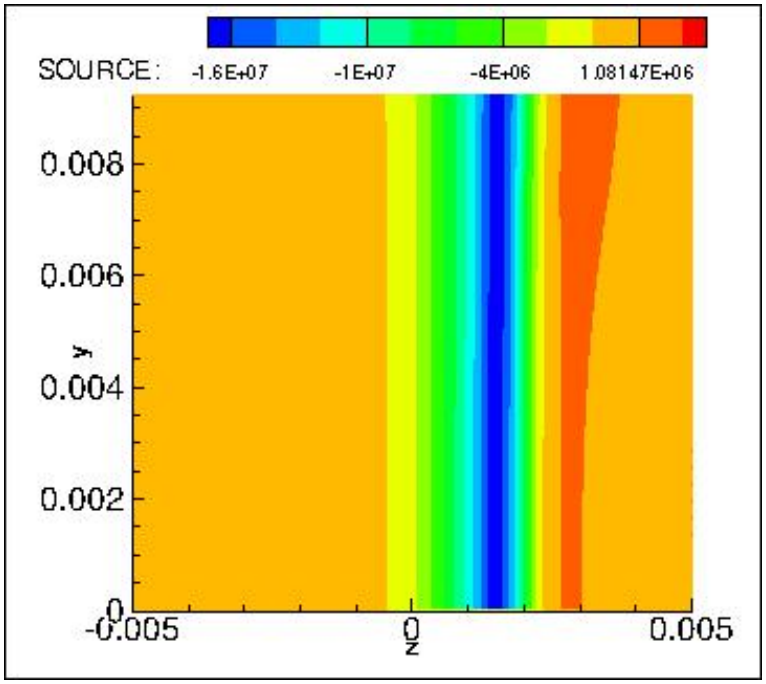

Figura 0.1: Profilo della divergenza dei flussi radiativi in una fiamma a contro-diffusione $CH_4 - O_2/CO_2$, $[Jm^{-3}s^{-1}]$.

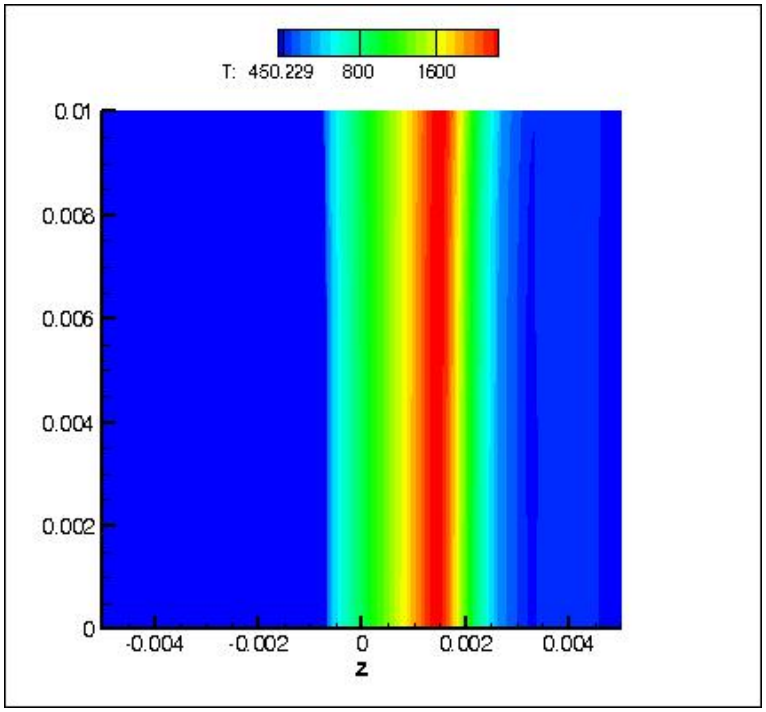

Figura 0.2: Soluzione della fiamma laminare a contro diffusione O_2/CO_2.

Come si può facilmente notare tale termine è negativo nelle zone ad alta temperatura (la fiamma perde energia a vantaggio di zone più fredde), mentre risulta essere positivo nelle zone più fredde e dove è presente una elevata concentrazione di CO_2 ($z > 0.002\,m$). Tale soluzione è stata ottenuta avanzando le equazioni con un dt di $2*10^{-14}$, di 50000 volte più grande rispetto al tempo di avanzamento consentito da un metodo completamente esplicito quale il Runge-Kutta al terzo ordine di Shu ed Osher.

1 The RTE model

Radiation hydrodynamics plays an important role in astrophysics, laser fusion, plasma physics and combustion. For many years, efforts have been underway to develop mathematical models and numerical schemes to obtain accurate predictions at reasonable computing cost in this domain. One of the main difficulty is to obtain accurate numerical computations in the various regimes that can be encountered due to values of material opacities which can vary from several order of magnitude. This can be achieved by using the full radiative transfer equation but it is still out of range for complex simulations in particular in two or three spatial dimensions. To overcome this difficulty several models have been derived. For large values of the material opacity, an asymptotic analysis leads to hyperbolic/parabolic systems of equation referred to as the equilibrium-diffusion limit or non equilibrium diffusion approximation ([12]). On the other hand, for smaller values of the opacity the streaming limit can be handled by using an hyperbolic system of equations coupling some closure of the moment system of the transfer equation with the hydrodynamic system ([1],[2]) . In this paper we propose new model and numerical scheme to describe radiation hydrodynamics in a wide range of regimes. The equations for the fluid are the classical conservation laws (mass, momentum and energy). The radiation is described by the grey moment system of the transfer equation (radiative energy and radiative flux) with the M_1 closure introduced in ([3][4]). This closure, based on the minimum entropy principle, is able to describe large anisotropy of the radiation while giving also the correct diffusion limit. The Eddington factor is a non constant function of the reduce flux and therefore the radiation subsystem is a nonlinear hyperbolic system. Here, these equations are written in the comoving frame, introducing some non conservative coupling terms. A Riemann solver is developped by performing a wave decomposition neglecting the nonconservative coupling terms and the source terms, which is trivial since the two subsystems then decouple. Afterwards the nonconservative terms are reintroduced in the scheme, by using in the radiation equations the velocity given by the hydrodynamic solver. This approach, natural in the streaming regime, can be improved to capture the diffusion limit. For that purpose the Riemann solver for the M_1 subsystem is modified to take into account the stiff relaxation term along the ideas developed in ([5]). In the next section we give the equations of radiation hydrodynamics with the M1-closure, then we present the numerical methods for solving these equations and at the end we present a simple numerical experiments in a counter diffusion laminar flame of $CH_4 - O_2/CO_2$.

1.0.1 The M_1 Physical Model

The equations of grey radiative hydrodynamics under the assumption of local thermodynamic equilibrium are:

$$\frac{\partial E_r}{\partial t} + \nabla \cdot \boldsymbol{F_r} = c(\sigma_P a T^4 - \sigma_E E_r). \tag{1.1}$$

ed una equazione di trasporto per il suo flusso F ($Jm^{-2}s^{-1}$):

$$c\frac{\partial F_r}{\partial t} + c\nabla \cdot \boldsymbol{D_r} E_r = -\sigma_F \boldsymbol{F_r}. \tag{1.2}$$

In order to close system (1.1 − 1.2) it is necessary to give two equations of state for the radiation. We need a closure relation giving the radiative pressure Pr in term of the radiative energy Er and of the radiative flux Fr. A rather simple closure is to assume that the radiative flux is isotrope which leads to the closure Pr = 1/3Er. . Such an approximation is by construction not very well suited to model flow containing large anisotropy in the radiative flux which is generally the case for radiative shocks. We will therefore use the closure given by the M_1 model. In this model, the radiative pressure is given by:

$$\boldsymbol{P_r} = \boldsymbol{D} E_r. \tag{1.3}$$

where the Eddington tensor **D** is defined by:

$$\boldsymbol{D} = \frac{1-\chi}{2}\boldsymbol{I} + \frac{3\chi - 1}{2} n \otimes n. \tag{1.4}$$

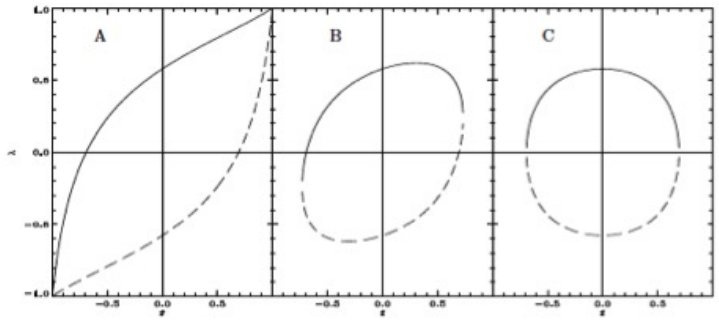

Figura 1.1: eigenvalues of M_1, $\frac{\lambda^+}{c}$ (full line) and $-\frac{\lambda^-}{c}$ (dashed line) according to $f = F_r/(cE_r)$.

$$\chi = \frac{3 + 4|f|^2}{5 + 2(4 - 3|f|^2)^{0.5}}. \tag{1.5}$$

$\boldsymbol{I}$ is the identity matrix, χ the Eddington factor, f = Fr/cEr the reduce flux and n = f/|f| is a unit vector aligned with the radiative flux. The previous system is a hyperbolic one which can be written under the following form:

$$\partial_t U + \partial_x F(U) = S(U) \tag{1.6}$$

with

$$J(U) = \frac{\partial F(U)}{\partial U} = \begin{pmatrix} 0 & 1 \\ c^2(\chi(f) - \chi^{'}(f)f) & c\chi^{'}(f) \end{pmatrix} \tag{1.7}$$

The eigenvalues, $\lambda-$ and $\lambda+$, of J are plotted in Fig. 1.1. At radiative equilibrium (when f = 0), the eigenvalues are equal to $\pm c/\sqrt{3}$, which is a direct consequence of the isotropy of underlying distribution function of the photons. On the other hand, in the case of extreme non-equilibrium, when f = 1 (resp. f = −1), the eigenvalues are degenerated and are equals to c (resp. −c). This case corresponds to the free-streaming limit where all the photons move towards the same direction. It is important to note that in the case of a constant Eddington factor ($\chi = 1/3$), the eigenvalues are also constant and equal to $\pm c\sqrt{3}$, which means that a light front can not propagate at the speed of light, as it should. It is worth noticing that the wave speeds of this subsystem, which mathematically correspond to the eigenvalues of its Jacobian matrix (1.7), depend only on the norm of the reduced flux f and on the angle θ of this flux with the considered interface. These wave speeds describe the speed at which the information is transported in the system, in the same way as the sound speeds in a fluid at rest.

Fig. 1.1 illustrates the behavior of the eigenvalues normalized by c for some characteristic values of θ and f. The left plot corresponds to a flux perpendicular to the interface ($\theta = 0$), which is similar to the mono-dimensional problem. In particular, for a unit reduced flux (points A), the four eigenvalues are equal to c so the transport limit is correctly described. The middle plot represents the case where the flux is parallel to the interface. In that particular case, two eigenvalues are always equal to zero and the two others are equal in norms but of opposite sign. We can also notice that, when the reduced flux is unity (points C), the four eigenvalues™ are null. This is particularly interesting because it corresponds to the physical characteristic speeds of a transverse flux and because it means that there is no transport perpendicular to the radiative flux. In all cases, we find that for f = 0 (points B), the eigenvalues are $(\frac{-c}{\sqrt{3}}, 0, 0, \frac{c}{\sqrt{3}})$, which are the proper propagation speeds in the diffusion limit. The system (1.1-1.2) can be discretized using a Godunov method based on the HLLE approximate Riemann solver. Hence, we need to find an estimation of the largest and smallest physical signal-velocities in the exact solution to the Riemann problem. This estimation involves the eigenvalues of the Roe's linearization for the M_1 model. The M_1 Roe's matrix $J_{i+1/2}$ between i and i+1 states can be written as:

$$J_{i+1/2} = \begin{pmatrix} 0 & 1 \\ (\chi_a - \chi_m^{'} f_a) & \epsilon\chi_m^{'} \end{pmatrix} \tag{1.8}$$

where the subscript a indicates the state between i and i + 1 states. The eigenvalues $\lambda^{\pm}_{i+1/2}$ of this matrix are:

$$\tilde{\lambda}^{\pm}_{i+1/2} = (\epsilon\chi^{'}_{m} \pm \sqrt{(\epsilon\chi^{'}_{m})^2 + 4(\chi_a - f_a\chi^{'}_{m})})/2 \tag{1.9}$$

One can give an estimation of the largest and smallest physical signal velocities:

$$\tilde{a}^{+} = max(\tilde{\lambda}^{+}_{i+1}, \tilde{\lambda}^{+}_{i+1/2}, 0);\ \tilde{a}^{-} = min(\tilde{\lambda}^{-}_{i+1}, \tilde{\lambda}^{-}_{i+1/2}, 0); \tag{1.10}$$

Using the HLLE solver gives the following expressions for the flux:

$$\tilde{F}_{r,i+1/2} = \frac{\tilde{a}^{+}\tilde{F}_{r,i} - \tilde{a}^{-}\tilde{F}_{r,i+1}}{\tilde{a}^{+} - \tilde{a}^{-}} + \frac{\tilde{a}^{+}\tilde{a}^{-}}{\tilde{a}^{+} - \tilde{a}^{-}}(E_{r,i+1} - E_{r,i}); \tag{1.11}$$

$$P_{r,i+1/2} = \frac{\tilde{a}^{+}P_{r,i} - \tilde{a}^{-}P_{r,i+1}}{\tilde{a}^{+} - \tilde{a}^{-}} + \frac{\tilde{a}^{+}\tilde{a}^{-}}{\tilde{a}^{+} - \tilde{a}^{-}}(\tilde{F}_{r,i+1} - \tilde{F}_{r,i}); \tag{1.12}$$

Rewritting the system in the original variables, we get the following discretization for the M_1 model:

$$\frac{1}{\Delta t}(E^{n+1}_r - E^{n}_r)_i + \frac{1}{\Delta r}(F_{r,i+1/2} - F_{r,i-1/2})^{n+1/2} = \sigma c(a_r T^4 - E_r)^{n+1/2}_i; \tag{1.13}$$

$$\frac{1}{\Delta t}(F^{n+1}_r - F^{n}_r)_i + \frac{c^2}{\Delta r}(\hat{P}_{r,i+1/2} - \hat{P}_{r,i-1/2})^{n+1/2} = -\sigma c F_{r,i})^{n+1/2}_i; \tag{1.14}$$

where we have defined $\epsilon = \frac{1}{\sigma l}$, l being a characteristic length and:

$$\hat{P}_{r,i+1/2} = \epsilon^2 P_{r,i+1/2} + (P_{r,i+1} + P_{r,i})/2 \text{ and } F_{r,i\pm1/2} = c\epsilon\tilde{F}_{r,i\pm1/2}; \tag{1.15}$$

In the previous discretization of the radiation subsystem, one need the value of ϵ at each interface. In practical computations, where the opacity gradient can be large, we compute a value in each cell $\epsilon = 1/\sigma\Delta x$. The value of ϵ at the interface is then taken to be the maximum value in the two adjacent cells. As we will see this method has given very satisfactory results even in the case of radiative shock with very strong opacity gradient. Nevertheless using HLLE solver for the radiation insures positivity of the scheme.

1.0.2 Super-Convergent Implicit-Explicit Peer Methods with A-stable Implicit Part

In this section we briefly describe the numerical method adopted for solving the Eqs. 1.1-1.2 that are of the form:

$$u' = F_0(u) + F_1(u) \tag{1.16}$$

where F_0 is a non-stiff or mildly stiff part and F_1 is a stiff contribution, arise in many initial value problems. Such problems often result from semi-discretized systems of partial differential equations with diffusion, advection and reaction terms. Implicit-explicit (IMEX) methods use this decomposition by treating only the F_1 contribution in an implicit fashion. The advantage of lower costs for explicit schemes is combined with the favourable stability properties of implicit schemes to enhance the overall computational efficiency. The resulting IMEX scheme is:

$$w_n = Pw_{n-1} + \Delta t\tilde{Q}F_0(w_{n-1}) + \Delta t\tilde{R}F_0(w_n) + \Delta tQF_1(w_{n-1}) + \Delta tRF_1(w_n) \tag{1.17}$$

Here, $\tilde{Q}, \tilde{R}, Q, R$ are the coefficient matrix of the PEER scheme of order s + 1 with s = 4 the steps of the scheme [6].

2 Numerical experiment: the 2D $CH_4 - O_2/CO_2$ counter diffusion flame

To validate the efficiency and stability of the scheme adopted to solve Eqs. 1.1-1.2 we apply the method to a counter diffusion flame of $CH_4 - O_2/CO_2$. The configuration of this type of flame is shown in Fig.2.1. where the oxidizer is $Y_{CO_2} = 0.763, Y_{O_2} = 0.237$ and the fuel is pure CH_4. We simulated the positive plane

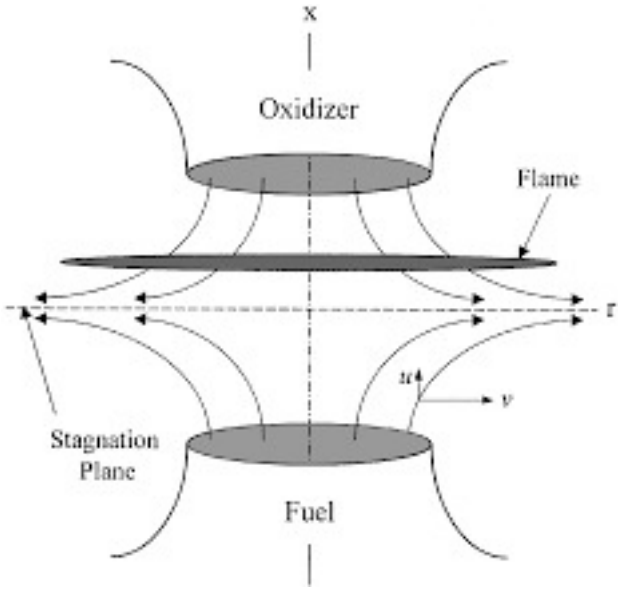

Figura 2.1: Scheme of a counter diffusion flame.

r > 0 of Fig.2.1 due to the simmetry with respect to x line. The velocity of the pure CH_4 is $1\,ms^{-1}$ and the oxidizer has the same momentum. The Planck mean absorption coefficient for CO_2, H_2O, CO, CH_4 with the HITRAN software [7] and as an example the value of the coefficient of the CO as a function of temperature and pressure is shown in Fig. 2.2: As shown in Fig. 2.2a-b, the Planck mean absorption coefficient σ_P vary with

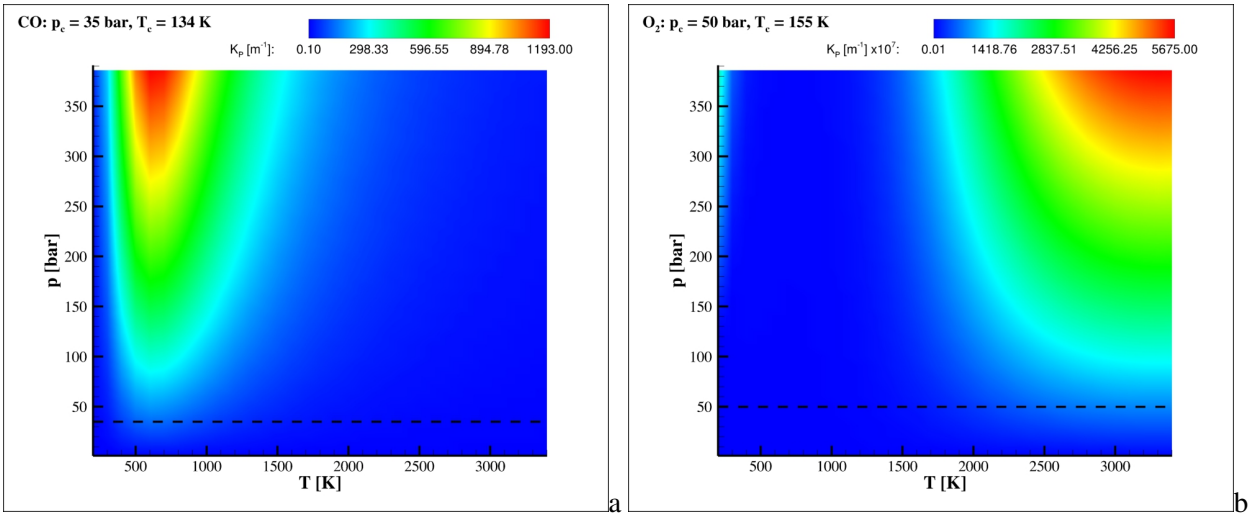

a b

Figura 2.2: a) CO and b) O_2 Planck mean absorption coefficient as a function of temperature [K] and pressure [bar].

temperature and pressure. At high pressure this coefficient can be greater than 50 times that at atmospheric

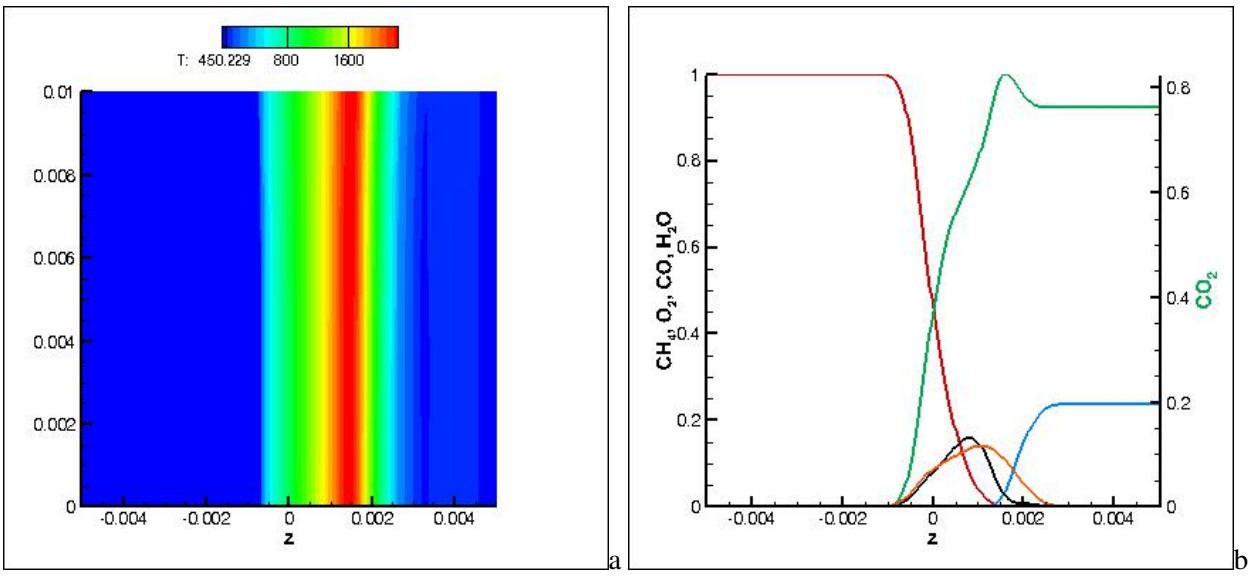

Figura 2.3: a) Temperature profile of the counter diffusion flame; b) Species profile at y = 0.

pressure as shown in Fig.2.2a. The temperature profile is not uniform along y, since the velocity strain rate is not constant as a function of y (see Fig.2.3a). Fig. 2.3b shows the mean species profiles at y = 0 of maximum velocity strain. The combustion products are formed near the stagnation plane at a value of z ~ 0.0015 where the temperature reachs a maximum value of approximately $2250K$. Regarding the schematic configuration of Fig. 2.1, we simulate, due to simmetry, the plane x − r with r > 0 and y axis in the simulations corresponds to r. Fig. 2.4a shows Radiative Energy results of our simulation for the counter diffusion flame. It reachs its

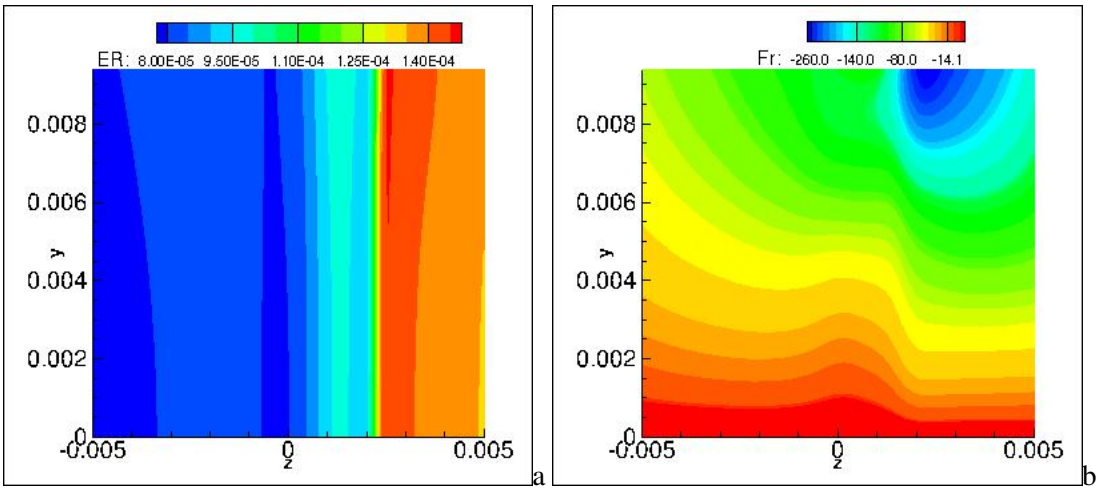

Figura 2.4: a) Radiation Energy profile of the counter diffusion flame; b) F_y Radiation Flux.

maximum value at positive z where the CO_2, a strong absorber, mass fraction has a peak (see green line in Fig.2.3b) and temperature starts to decrease from its maximum value. In fact seeing at the divergence of the radiative fluxes in Fig.2.4d (Source = $\Delta \cdot \boldsymbol{F}$) we observe that the total energy equation presents a sink where the flame reachs its peak 2254K and a source where the temperature decreases towards the inlet temperature 450K. So the primary effect of radiation is to decrease the zone of the flame at higher temperature (by approximately 60K) and increase that at the inlets where CO_2 is present. The solution of the Eqs. 1.1-1.2 is stably obtained with the new IMEX-PEER method of 5^{th}, s = 4 order with a maximum Δt of the order of $2 * 10^{-14}$s. The total simulated time is $2 * 10^{-9}$s and it takes approximately 100000 iterations to reach the steady state solution.

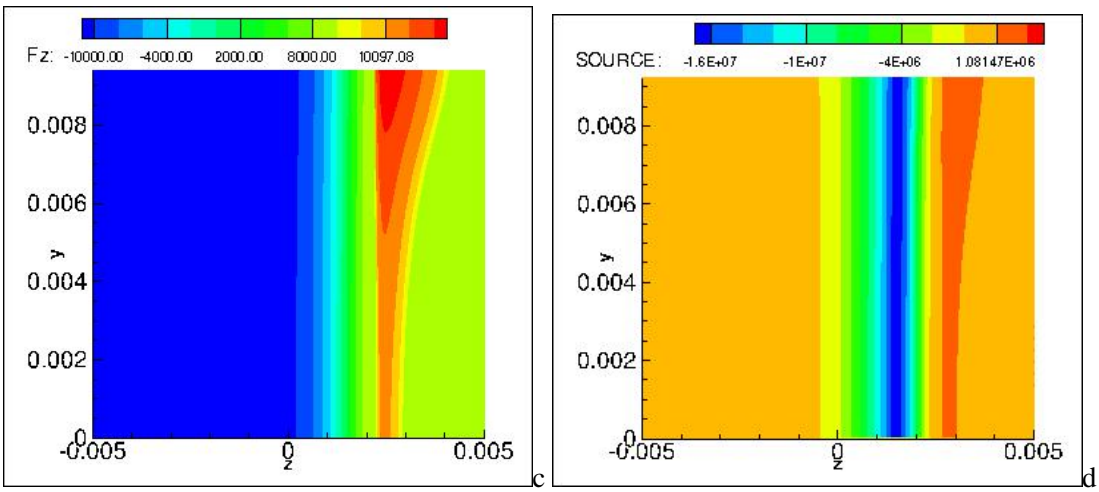

Figura 2.5: a) F_z Radiation Flux; b) Radiation Energy source term profile of the counter diffusion flame.

2.1 Conclusions

In this work we have implemented in the code HeaRT a new and efficient numerical model (IMEX-PEER) for solving the radiative transfer equations. The radiative transfer is solved using a moment method and the M_1 closure relation. This method gives satisfactory results in a wide range of physical conditions including both the diffusion and the free-streaming regimes where the anisotropy of the photons distribution function can be large. To numerically solve the thermal Radiation system of equation, we use a second-order Godunov type algorithm for the hyperbolic subsystem. The partial Riemann solver used to obtain the numerical fluxes is a HLLE (Harten-Lax-van Leer-Einfeldt) scheme. Works are in progress to incorporate in the model equations the effect of turbulence. The IMEX-PEER numerical method allows us to stably advance the equation with a $\Delta t = 2 * 10^{-14}$ s, 20000 times greater tha a classical Runge-Kutta method.

Acknowledgments

The computing resources and the related technical support used for this work have been provided by CRESCO/ENEAGRID High Performance Computing infrastructure and its staff [8]. CRESCO/ENEAGRID High Performance Computing infrastructure is funded by ENEA, the Italian National Agency for New Technologies, Energy and Sustainable Economic Development and by Italian and European research programmes (see http://www.cresco.enea.it/english for information).

Bibliografia

[1] G. C. Pomraming. *The Equations of Radiation Hydrodynamics*. C.R. Acad. Sci., 1973.

[2] J. E. Morel R. B. Lowrie and J. A. Hittinger. The Coupling of Radiation and Hydrodynamics. *The Astrophys. J.*, 521:432–450, 1999.

[3] B. Dubroca and J.-L. Feugeas. *Etude Theorique et Numerique d'une Hierarchie de Modelles aux Moments pour le Transfert Radiatif*. C.R. Acad. Sci., 1999.

[4] J.R. Howell, R. Siegel, and M.P. Menguc. *Thermal Radiation Heat Transfer*. CRC Press, Taylor & Francis Group, 5th edition, 2010.

[5] L. Pareschi et G. Toscani S. Jin. Uniformly accurate diffusive relaxation schemes for multiscale transport equations. *SIAM J. Num. Anal.*, 38(913), 2000.

[6] W. Hundsdorfer M. Schneider, J. Lang. Extrapolation-based super-convergent implicit-explicit Peer methods with A-stable implicit part. *J. Comp. Physics*, 367:121–133, 2017.

[7] L.S. et al. Rothman. The HITRAN 2008 Molecular Spectroscopic Database. *J. of Quantitative Spectroscopy and Radiative Transfer*, 110:533–572, 2009.

[8] Ponti G. et al. The role of medium size facilities in the HPC ecosystem: the case of the new CRESCO4 cluster integrated in the ENEAGRID infrastructure. In *Proceedings of the 2014 International Conference on High Performance Computing and Simulation*, volume HPCS 2014, pages 1030–1033, 2014.